Title: Rod nuclear architecture determines contrast transmission of the retina and behavioral sensitivity in mice

Authors:

Kaushikaram Subramanian[1,2], Martin Weigert[1,2], Oliver Borsch[3], Heike Petzold[1], Alfonso García-Ulloa [1], Eugene Myers[1,2,4], Marius Ader[3], Irina Solovei[5], Moritz Kreysing[1,2,*]

Affiliations:

1) Max Planck Institute of Molecular Cell Biology and Genetics, Dresden
2) Center for Systems Biology Dresden, Dresden
3) Center for Regenerative Therapies Dresden, Technische Universität Dresden
4) Department of Computer Science, Technische Universität Dresden
5) Biozentrum, Ludwig Maximilians Universität, München

(*) kreysing@mpi-cbg.de

Abstract:

Rod photoreceptors of nocturnal mammals display a striking inversion of nuclear architecture, which has been proposed as an evolutionary adaptation to dark environments. However, the nature of visual benefits and underlying mechanisms remains unclear. It is widely assumed that improvements in nocturnal vision would depend on maximization of photon capture, at the expense of image detail.

Here we show that retinal optical quality improves 2-fold during terminal development, which, confirmed by a mouse model, happens due to nuclear inversion. We further reveal that improved retinal contrast-transmission, rather than photon-budget or resolution, leads to enhanced contrast sensitivity under low light condition. Our findings therefore add functional significance to a prominent exception of nuclear organization and establish retinal contrast-transmission as a decisive determinant of mammalian visual perception.

One Sentence Summary:

Our study reveals that chromatin compaction in rod cells augments contrast sensitivity in mice.

Introduction

The structure of the vertebrate retina requires light to pass through multiple cell layers prior to reaching the light-sensitive outer segments of the photoreceptors (Dowling, 1987). In nocturnal mammals, the increased density of rod photoreceptor cells demands a thicker (Němec et al., 2007; Peichl, 2005) rod nuclei-containing outer nuclear layer (ONL). For mice, where rods account for around 80% of all retinal cells (Hughes et al., 2017), this layer of photoreceptor nuclei is 55±5μm thick, thus creating an apparent paradox by acting as a more pronounced barrier for projected images prior to their detection (Fig. 1A). Interestingly, rod nuclei are inverted in nocturnal mammals (Błaszczak et al., 2014; Kreysing et al., 2010; Solovei et al., 2009; 2013), such that heterochromatin is detached from the nuclear envelope and found in the nuclear center, whereas the less-dense euchromatin is re-located to the nuclear periphery. Given that this nuclear inversion is exclusive to nocturnal mammals and correlates with the light-focusing capabilities of isolated nuclei, it was proposed as an evolutionary adaptation to life under low-light conditions (Błaszczak et al., 2014; Kreysing et al., 2010; Solovei et al., 2009). However, the nature of any visual improvements that could arise from nuclear inversion remains unclear.

It is widely assumed that high-sensitivity vision depends on optimized photon capture (Schmucker and Schaeffel, 2004; Warrant and Locket, 2004) and often comes at the expense of image detail (Cronin et al., 2014; Warrant, 1999). Here, we show that nuclear inversion affects a different metric of vision, namely contrast sensitivity under low-light conditions. In particular, we experimentally show that nuclear inversion improves retinal contrast transmission, rather than photon capture or resolution. Advanced optical modelling and large-angle scattering measurements indicate that this enhanced contrast transfer emerges from previously coarse-grained (Błaszczak et al., 2014; Kreysing et al., 2010; Solovei et al., 2009) changes in nuclear granularity, namely a developmental reduction of chromocenter number (Fig. 1B1). Moreover, genetic interventions to change chromocenter number in adult mice reduces contrast transmission through the retina, and compromise nocturnal contrast sensitivity accordingly. Our study therefore adds functional significance to nuclear inversion by establishing retinal contrast transmission as a decisive determinant of mammalian vision.

Results

Volume specific light scattering from chromocenters

To test how the presence of densely packed rod nuclei in the light path affects the propagation of light through the retina, we compared transmission of micro-projected stripe images through freshly excised retinae of wild type (WT) (Fig. 1A) and Rd1/Cpfl1 KO mice(Chang et al., 2002), which lack all photoreceptors including the ONL (Fig. 1B2). In the absence of photoreceptors and their nuclei, we observed 49% greater imaged detail (cut-off chosen at 50% residual contrast, Fig. 1B3). Since photoreceptor nuclei contain highly compacted and molecularly dense DNA with significant light-scattering potential (Drezek et al., 2003; Marina et al., 2012; Mourant et al., 2000), while photoreceptor segments have been described as image-preserving waveguides (Enoch, 1961), these findings suggest that light propagation in the mouse retina is significantly impacted, if not dominated, by the highly abundant rod nuclei of the ONL.

We then asked whether retinal cell somata are optically specialized with distinct light scattering properties. A comparison of light scattering by different cell types using high throughput FACS(Feodorova et al., 2015) measurements revealed that isolated retinal cells scatter substantially less light than neurons of the brain and cultured neuroblastoma cells (Fig. 1C). This trend is seen for forward-scattered light but is even more pronounced for side scattering, which reflects subcellular heterogeneity. Using forward scattering as a measure of cell size indicates that side scattering normalized by volume is also noticeably lower in retinal cells (Fig. 1C, inset). This suggest that retinal cells are indeed optically specialized, as they scatter less light for a given size.

To determine when the low sideward light scattering characteristic of retinal nuclei emerges, we compared the scattering profile of retinal nuclei in P25 pups and adult (12 weeks) mice. We found little or no difference between forward light scattering (Fig. 1D-E), as predicted by earlier models (Błaszczak et al., 2014; Kreysing et al., 2010; Nagelberg et al., 2017). In stark contrast, however, side scattering (measured in a narrow range around 90°), with a strong potential to diminish image contrast, was

significantly reduced in adult retinal nuclei compared to the intermediate developmental stage (Fig. 1F). Quantitative analysis of sorted nuclei from P25 retinae further revealed a monotonic relation between chromocenter number and side scattering signal (Fig. 1G). In particular, those nuclei with the lowest number of chromocenters were found to scatter the least. In support of this experimental quantification, a wave-optical Mie model of light-scattering by refractive chromocenters closely reproduced the trend of light scattering reduction with chromocenter fusion (Fig. 1H).

To establish whether rod nuclear inversion is required to cause the developmental reduction in light scattering, we used a transgenic mouse model (TG-LBR) in which heterochromatin remains anchored at the lamina which in turn prevents the complete fusion of chromocenters (Fig. 2A1, A2 , 2B, Fig. S2)(Solovei et al., 2013). FACS experiments of nuclei from TG-LBR retinae, in which >70% of the nuclei are successfully arrested (Fig. S4), revealed significantly increased light scattering (Fig. 2C, Fig. 1F). Specifically, the global maximum of the side-scattering was re-located precisely to the position that is characteristic of nuclei isolated from WT pups at P14, which possess a similar number of chromocenters as inversion arrested nuclei (compare Fig. 2B, C, Fig. 1F, G). Because inhibition of chromocenter fusion leads to specific increase in scattering, we conclude that the reduction of light scattering with chromocenter number is causal.

Improved retinal contrast transmission

Next, we asked how nuclear substructure could affect the optical properties of the ONL. We first approached this via a simulation that built on recent advances in computational optics (Weigert et al., 2018). This allowed us to specifically change nuclear architecture, while leaving all other parameters, including the morphology and relative positioning of about 1750 two-photon mapped nuclei, unchanged (Fig. 2D1) (Supplementary Methods).

These simulations suggested that especially the sideward scattering (cumulative scattering signal at angles >30 deg) monotonically decreases when 10 chromocenters successfully fuse into one (Fig. 2D2, 2E). Physically, this effect of

135 reduced scattering can be explained by a reduction of volume-specific scattering for weak scatterers in the size regime slightly above one wavelength of light, similar to scattering reduction techniques proposed for transparent sea animals(Johnsen, 2012) (Fig. 2 F, G). Furthermore, a minimal optical ONL model reconstituted from suspended beads of different size but same volume fraction (Supplementary
140 Methods) illustrates how a decreased geometric scattering cross section after fusion leads to reduced scattering-induced veil that helps to prevent contrast losses (Fig. 2H and inset). Taken together these data suggest that nuclear inversion might serve to preserve contrast in retinal transmitted images.

145 To experimentally quantify the optical quality of the retina with respect to nuclear architecture, we applied the concept of the modulation transfer function (MTF), a standard way to assess image quality of optical instruments (Boreman, 2001). Specifically, MTF indicates how much contrast is maintained in images of increasingly finer sinusoidal stripes (Fig. S5 B, C). We therefore devised an automated optical
150 setup (Fig. S5 A) that allowed us to project video sequences of demagnified sinusoidal stripe patterns through freshly excised retinae and assess the retinal transmitted images for contrast loss. This custom built set-up mimics the optics of the mouse eye, in particular its f-number (Schmucker and Schaeffel, 2004), while circumventing changes of the optical apparatus in-vivo (Fig. S5, Supplementary
155 Materials & Methods).

Strikingly, we found that wildtype retinae improve contrast transmission throughout terminal development, with adult retinae showing consistently elevated MTFs compared to intermediate developmental stages (P14) in which rod nuclei still
160 possess around 5 chromocenters (Fig 3A). In contrast to many lens-based optical systems, retinal MTFs do not display a strict resolution limit. Instead a monotonic decay of retina transmitted contrast indicates scattering induced veil, rather than a frequency cut-off to be the cause of contrast loss (Fig. 3 A, B Fig. S6 A-D). Collected from >1300 high resolution images, this data reveals that, similar to the lens
165 (Tkatchenko et al., 2010), the retina matures towards increasing optical quality during

latest developmental stages, with chromocenter fusion as a putative mechanism of veil reduction.

Next, we asked if developmental improvements in contrast transmission of the retina are indeed caused by chromocenter fusion. For this we used mice in which LBR-overexpression largely arrested chromocenter fusion, resulting in an elevated number of chromocenters in the adult animal, similar to P14 WT (Fig. 2A2 2B), without displaying any effect on other morphological characteristics (Fig. S4). Strikingly, repeating MTF measurements on adult retinae of this inversion arrested mouse model (TG-LBR), we find near identical contrast attenuation characteristics as in the developing retina (compare Figs. 3A and 3B). Thus, developmental improvements of retinal contrast transmission are indeed mediated by the inversion of rod nuclei.

Frequently, the quality of image-forming optical systems is reported as a single parameter value called the Strehl ratio (Thibos et al., 2004). Since our image projection setup closely mimics the mouse eye, it allows meaningful comparisons of the Strehl ratios of retinae, by comparing the volumes under MTF curves. With regard to our MTF measurements, we that find the Strehl ratio of a fully developed retina is increased 2.00 ± 0.15-fold compared to that of pups (P14) in which chromocenters fusion was not completed, and similarly 1.91 ± 0.14-fold (ratio of means ± SEM) improved compared to TG-LBR adult retinae ($p<0.001$) in which chromocenter fusion was deliberately arrested (Fig. 3C).

Since the Strehl ratio makes predictions for the peak intensity of a tissue transmitted point stimulus, we analyzed the effect of micro-projecting a point-like stimulus through the mouse retina (diameter here ~3μm, measurement constrained by outer segment spacing). We found that the resulting image at the back of the WT retina had a near two-fold (1.79 ± 0.38, mean ± SD) higher peak intensity compared to the TG-LBR retina (Fig. 3D, N=119, N=121, measured in at a total of 6 animals). The full-width half maximum (FWHM) of the PSF, however, remained virtually unchanged (4.32±2.38 μm, 3.75±2.01 μm, mean ± SD for WT & TG-LBR retinae respectively). These measurements indicate that contrast is lost due to the generation of image veil from

side scattering, which overcasts attenuated, but otherwise unchanged signals. Accordingly, when comparing the integrated absolute transmission through rhodopsin-bleached retinae in dedicated experiments (Supplementary methods), we found near identical transmission values for WT and inversion arrested retinae (T_{WT} 74±8 %, T_{LBR} = 72 ±5 %, mean ±SD), which emphasizes that despite differential image signal, the overall photon arrival at the photoreceptor outer segments, remains unchanged.

The advantage of improved retinal contrast transmission becomes apparent not only when following the motion of individual (non-averaged) light stimuli that appear at considerably higher signal-to-noise levels (Fig. 3E) at the outer segments level, but also in a real-life example, when images of an approaching cat are micro-projected through a mouse retina (Fig. 3F). Nuclear inversion results in cat images becoming visible considerably earlier compared to mice that lack nuclear inversion (4 vs 3 meters, at a given arbitrary noise threshold). These results suggest that nuclear inversion may offer enhanced visual competence that originates from improved contrast preservation in retinal images.

Improved contrast sensitivity

To determine whether the improved retinal contrast transmission translates into improved visual perception, we carried out behavioral tests using *Opto-motor-reflex* measurements (Fig. 4A). Specifically, we used a fully automated mouse tracking and data analysis pipeline (Striatech technologies) (Benkner et al., 2013) to compare the contrast sensitivities of adult WT mice and those with arrested nuclear architecture (TG-LBR). Firstly, contrast sensitivity assessed by the animal's ability to detect moving stripes, did not differ significantly between the two genotypes at photopic light condition (70 Lux – the typical brightness of monitor). Transgenic and WT animals showed comparable visual sensitivity, as quantified by the area under the log-contrast sensitivity curve (AULC, Fig. 4B, left)(Villegas et al., 2002). As nuclear adaptation is strongly correlated with nocturnal lifestyle(Solovei et al., 2009; 2013), we adapted this set-up to assess contrast sensitivity under scotopic light conditions. At 20 mLux, which is the range of brightness in moonlight(Kyba et al., 2017), we again found comparable responses for coarse stimuli (wide large contrast stripes)

230 suggesting equally functional rod-based vision in TG-LBR and WT mice (Fig. 4B, right) without noticeable differences in absolute sensitivity. Furthermore, mice deficient of rhodopsin (*Rho*-/-) (Humphries et al., 1997; Jaissle et al., 2001) confirmed that visual behaviour under the displayed conditions fully relies on the functionality of the rod pathway (Fig. S7E).

235 When required to detect finer stripes, WT and TG-LBR mice displayed significant differences in their visual performance, specifically in contrast sensitivity (Fig. 4C). At 20mLux we observed an 18% greater AULC for WT mice compared with TG-LBR mice ($p < 0.01$). At even lower light intensities (2mLux, comparable to a starry night), the difference in AULC values was even greater (ratio 27%, $p< 0.01$) albeit at lower
240 absolute sensitivities, which agrees with reported values for WT mice (Alam et al., 2015; Prusky et al., 2004; 2000). The most significant differences in the contrast sensitivity occur above 0.15 cycles/degree (Fig. 4D). Especially, in the regime close to the visual acuity (0.26-0.30 cycles/degree), WT mice show up to 10 times ($p<0.0001$) greater positive response rates at intermediate contrasts (Fig. 4E)
245 compared to mice with inversion arrested rod nuclei. Moreover, at 90-100% contrasts, where WT mice approach a maximum responsiveness, we observed a near 6-fold reduced risk to miss a stimulus for WT compared to TG-LBR mice (false negative rates 11% WT, 59% TG-LBR).

Finally, we asked whether reduced visual sensitivity of mice lacking the inverted
250 nuclear architecture can be sufficiently explained by inferior contrast transmission of the retina. Direct comparison of behavioral sensitivity with the MTF curves showed that vision mostly occurs in regions in which retinal contrast transmission is higher than 50% and substantial differences in MTFs occur. Specifically, the 18-27% difference in contrast sensitivity goes together with a 26% higher Strehl ratio in WT
255 retinae when evaluated in the relevant frequency regime (0 - 0.36 cycles / degree). This suggest that at low light level contrast sensitivity is directly limited by contrast transmission through the retina, and that a reduction of contrast sensitivity in mice with non-inverted rod nuclei may be explained by increased contrast losses in the retina. Accordingly, matching the image contrast at the photoreceptor level of TG-
260 LBR mice with WT mice, while leaving intensities unchanged, should rescue contrast

sensitivity in TG-LBR mice. To test this, we first confirmed that contrast transmission through the inner retina is a linear process, with contrasts at the photoreceptor levels being proportional to contrasts in projected images (Fig. S7 B, C). We then adjusted the displayed contrasts in optomotor measurements to pre-compensate for higher contrast losses in the TG-LBR retina. Strikingly we found that with equal image contrast at the level of the photoreceptor segments, visual competence of LBR mice was rescued and becomes near identical to that of WT mice (Fig 4F). Thus, improved retinal contrast transmission sufficiently explains the augmented contrast sensitivity in mice with inverted rod nuclei.

Discussion

As an important determinant of fitness, animals evolved a wide range of visual adaptation to see in the dark (Nilsson, 2009; O'Carroll and Warrant, 2017; Thomas et al., 2017; Warrant and Nilsson, 2006; Warrant, 2017). Nocturnal vision is known to rely on highly efficient light capture, both at the level of the lens and photoreceptor outer segments, and often compromises spatio-temporal resolution by summation strategies of neuronal readout (Warrant, 1999; 2017). Here we established nuclear inversion as a complementary strategy to maximize sensitivity under low light conditions. Centrally, we show that it is the direction into which light is scattered inside retinal tissue that translates into differential contrast sensitivity. Specifically, we find that the forward scattering characteristic of inverted nuclei (Solovei et al., 2009, Kreysing et al., 2010) mainly suppresses light scattering by nuclear substructure towards large angles and image veil and contrast reduction resulting from it. As the mechanism involves improvements in retinal image contrast rather than notable changes in photon transmission that could impact absolute sensitivity (Banks et al., 2015; Cronin et al., 2014; Nilsson, 2009; Warrant, 1999), one might ask why nuclear inversion is an adaptation exclusive to nocturnal mammals. Wouldn’t improvements in retinal image contrast not also be beneficial for diurnal mammals? Firstly, the larger spacing of photoreceptor segments in the diurnal retina significantly reduces ONL thickness and thereby the risk of scattering induced veil and loss of image contrast. Furthermore, as is well known from photography, shot-noise that accounts for image granularity (Barlow, 1956; de Vries, 1943; Rose, 1948) becomes less of a problem with increasing light levels. Million-fold higher light intensities during

the day imply a higher safety margin from this noise floor (Warrant, 1999), (Fig. S7 F), as required for neural mechanisms of contrast enhancement to function (Artal et al., 2004; Flevaris and Murray, 2015; Hess and Dakin, 1988; Shevell et al., 1992). Such compensatory mechanisms are also likely to explain why no behavioral differences are observed at elevated intensities and why augmented vision becomes pronounced only at low light levels. Last, but not least, our measurements show that, although nuclear inversion improves retinal contrast transmission via reduced image veil, resolution, the limiting factor for high acuity diurnal vision, remains largely unaffected. In conclusion, our work adds functional significance to a prominent exception of an otherwise highly conserved pattern of nuclear organization and establishes retinal contrast transmission as a new determinant of mammalian fitness.

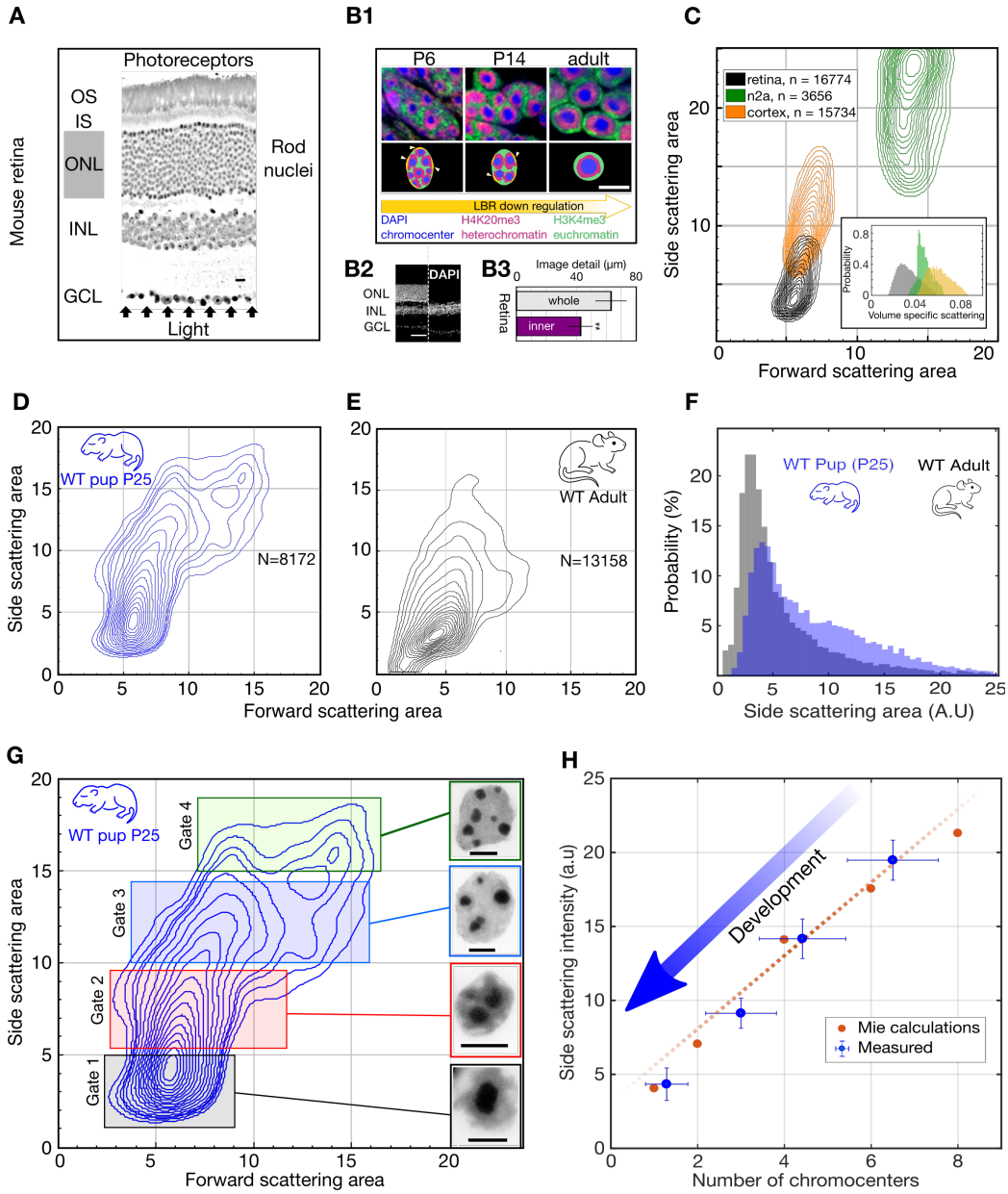

Fig. 1 Light scattering by retinal nuclei reduces with chromocenter number during development

(A) Longitudinal section showing the path of light through the mouse retina, including the rod nuclei dominated outer nuclear layer (ONL). Ganglion cell layer (GCL), inner nuclear layer (INL) and outer nuclear layer (ONL) and the inner and outer segments (IS & OS). **(B1) (top)** Downregulation of the lamina tether LBR (yellow) enables fusion of mobilized chromocenters and thereby an architectural inversion of mouse rod nuclei. **(bottom)** FISH images of rod nuclei stained with DAPI (blue) showing the dense chromocenters, LINE rich heterochromatin (H4K20me3, magenta) and SINE rich euchromatin (H3K4me3, green) **(B2)** DAPI section of WT mouse retina in comparison to a rd1-cpfl1 mouse retina showing the presence of only the inner retina. **(B3)** Quantification of image transmission shows that the inner retina alone (rd1-cpfl1, N=5) *transmits approximately 50% more image* detail than the full retina (N=11), suggesting significant image degradation in the thick outer nuclear layer. **(C)** FACS scattering profiles comparing retinal neurons, cortical neurons and N2a neuroblastoma cells and showing lower light scattering properties of retina neurons. (Inset) Volume specific light scattering is significantly reduced in the retina cell nuclei. **(D, E)** FACS scatter plot for isolated retinal nuclei from WT developmental stage week 3 pup (P25) and adult mice demonstrating stronger large angle scattering by the P25 nuclei. **(F)** Histogram of side scattering in adult and P25 retina depicting a higher side scattering for the developing retinal nuclei. **(G)** Sorting of developmentally maturing nuclei according to different side scattering signal. Insets show representative examples of Hoechst stained nuclei in the corresponding sort fractions. **(H)** Quantification of reduced scattering with chromocenter number is sufficiently explained by a wave optical model of light scattering n = 38 nuclei. (Error bars in **H** show s.d.) Scale bars **A** - 10 µm**. B1, G -** 5 µm, **B2** – 50µm

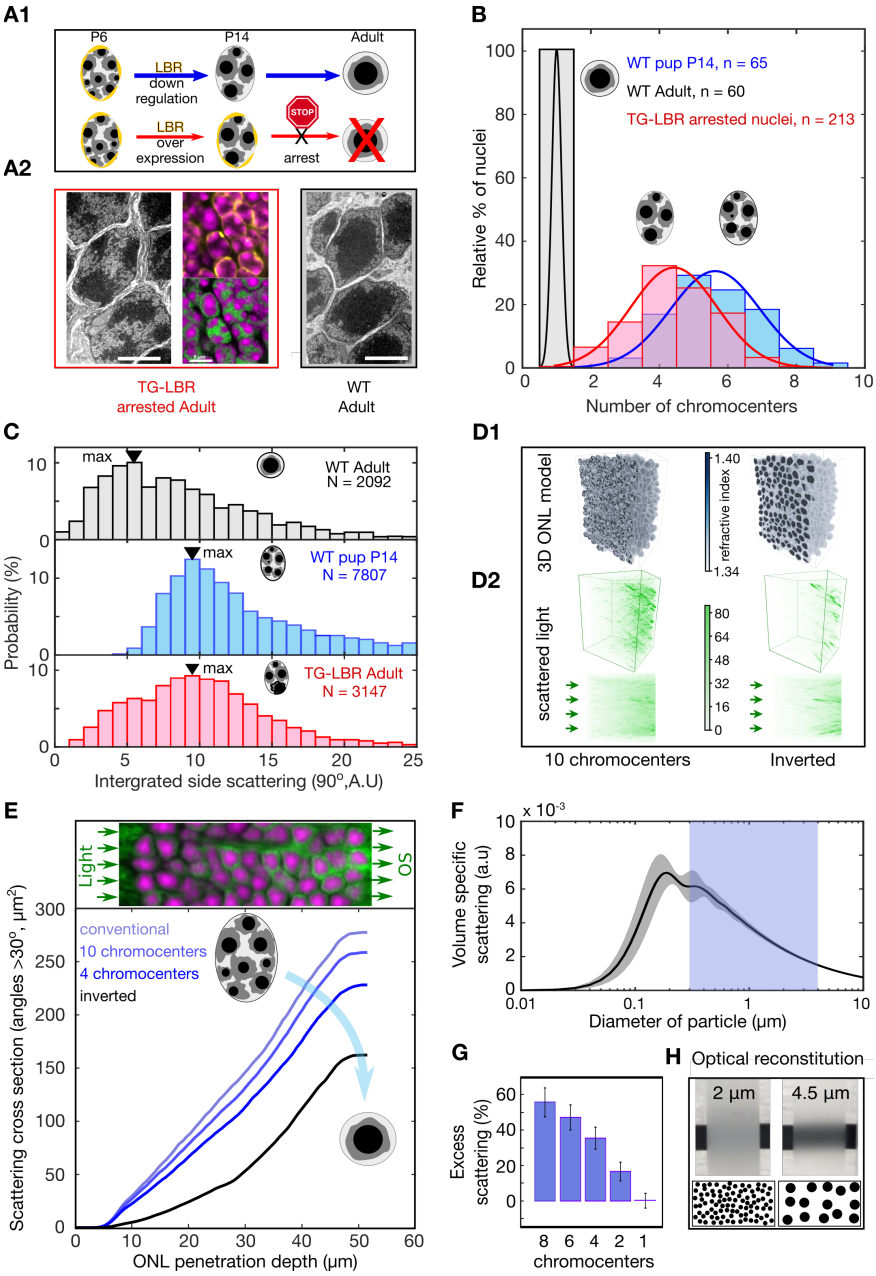

Fig. 2 Developmental arrest of chromocenter fusion increases light scattering from rod nuclei in measurements and tissue simulations. (A1) Schematic of the normal rod nuclear WT development and inversion arrested nuclei by LBR overexpression. **(A2)** EM images illustrating different electron densities in the euchromatic and heterochromatic phase underlying their refractive index (RI) differences (scalebar 5µm). (mid-top) Immunostaining of overexpressed of LBR tethers (yellow), and high-density heterochromatin (DAPI, magenta). (mid- bottom) Heterochromatic chromocenters (DAPI, magenta) and euchromatin (H4K5ac, green) **(B)** Chromocenter number distribution in LBR overexpressing rod nuclei is drastically different from WT mice, and similar to a developing WT pup (P14). **(C)** Side scattering assessed by FACS for TG-LBR retina nuclei is higher than that of WT nuclei and comparable to that of a WT P14 nuclei with similar chromocenter numbers. Note the shift of peak value upon LBR overexpression. **(D1)** 3d RI distribution mapped onto anatomically faithful volumetric ONL images. WT inverted architecture (right, top) and early developmental state (left) (simulation). **(D2)** (top) Differential simulations of light propagation in the ONL, using same positions and shapes of about 1750 nuclei, but varying chromatin distributions. (bottom) Maximum projection illustrating greater proportions of scattered light (angles >30deg) in the ONL with multiple chromo-centered nuclei. **(E)** Quantitative analysis of this data. **(F)** Angle weighted volume specific scattering strength for nuclei models evaluated by Mie scattering theory. **(G)** Excess scattering occurring in multi-chromocenter nuclei models. **(H)** Chromocenters scattering reconstituted in an emulsion of silica spheres in glycerol-water mixture. Pictograms reflect accurate number ratio of spheres.

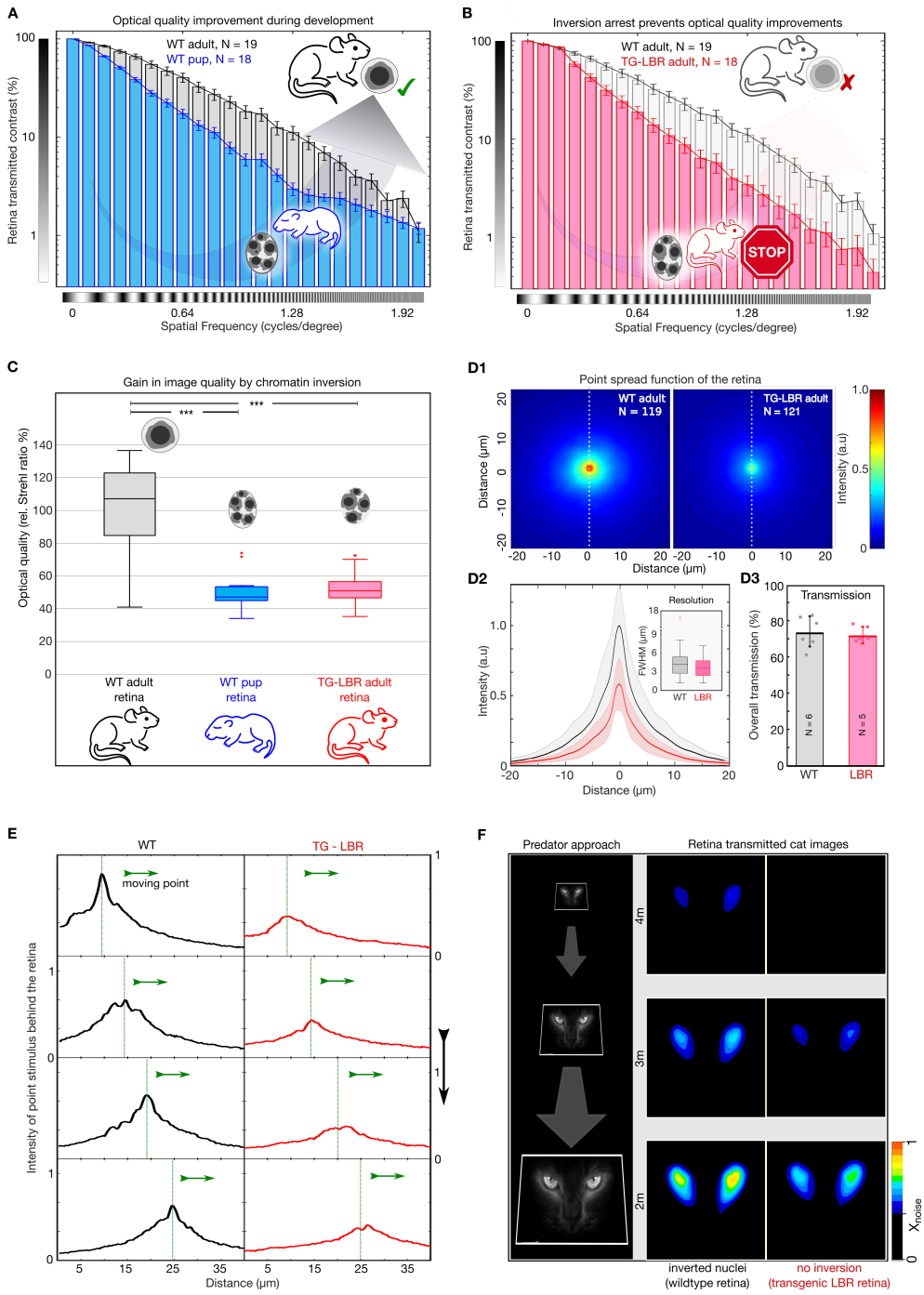

Fig. 3: Nuclear inversion improves retinal contrast transmission characteristics. **(A)** Retinal contrast transmission increases during developmental stages of nuclear inversion, as experimentally revealed by measurements of retina-transmitted sinusoidal stripe patterns (modulation transfer functions). Developmental stage P12-14 (N=18), compared to wildtype adult (N=19 animals), note log scale. **(B)** These improvements in optical quality do not occur in retinae in which rod nuclei are transgenitically arrested in development and maintain 4-5 chromocenters. TG-LBR mouse (N=18 animals) compared to WT reference (N=19 animals), N=1950 images in total. Mean +/- 95%CI. **(C)** The optical quality improvement of the retina (relative Strehl ratios), as caused by nuclear inversion, is two-fold ($p < 0.001$). **(D1)** Point spread function (PSF) for WT and LBR adult retinae by projection of 3um point light stimuli through the retina, N = 240 measurements in total 6 retinae. **(D2)** Intensity quantification along the white dotted line. Shaded region shows ± 1sd. Comparable resolution in transmitted images as assessed by the FWHM of the psf **(inset).** **(D3)** Near identical diffuse light transmission by both WT and TG-LBR retinae (n=2 animals each, mean ± s.d.) **(E)** Intensity of a moving, retina-transmitted point stimuli for WT (black) and TG-LBR mouse (red)**.** **(F)** Image-series of a cat approach as seen through the retina of mice, WT and transgenic genotype from various distances at the same vision limiting (arbitrarily chosen) signal to noise level. Consistent intensity differences of two or more color shades indicate significantly better predator detection potential for WT mice. Data magnified for clarity.

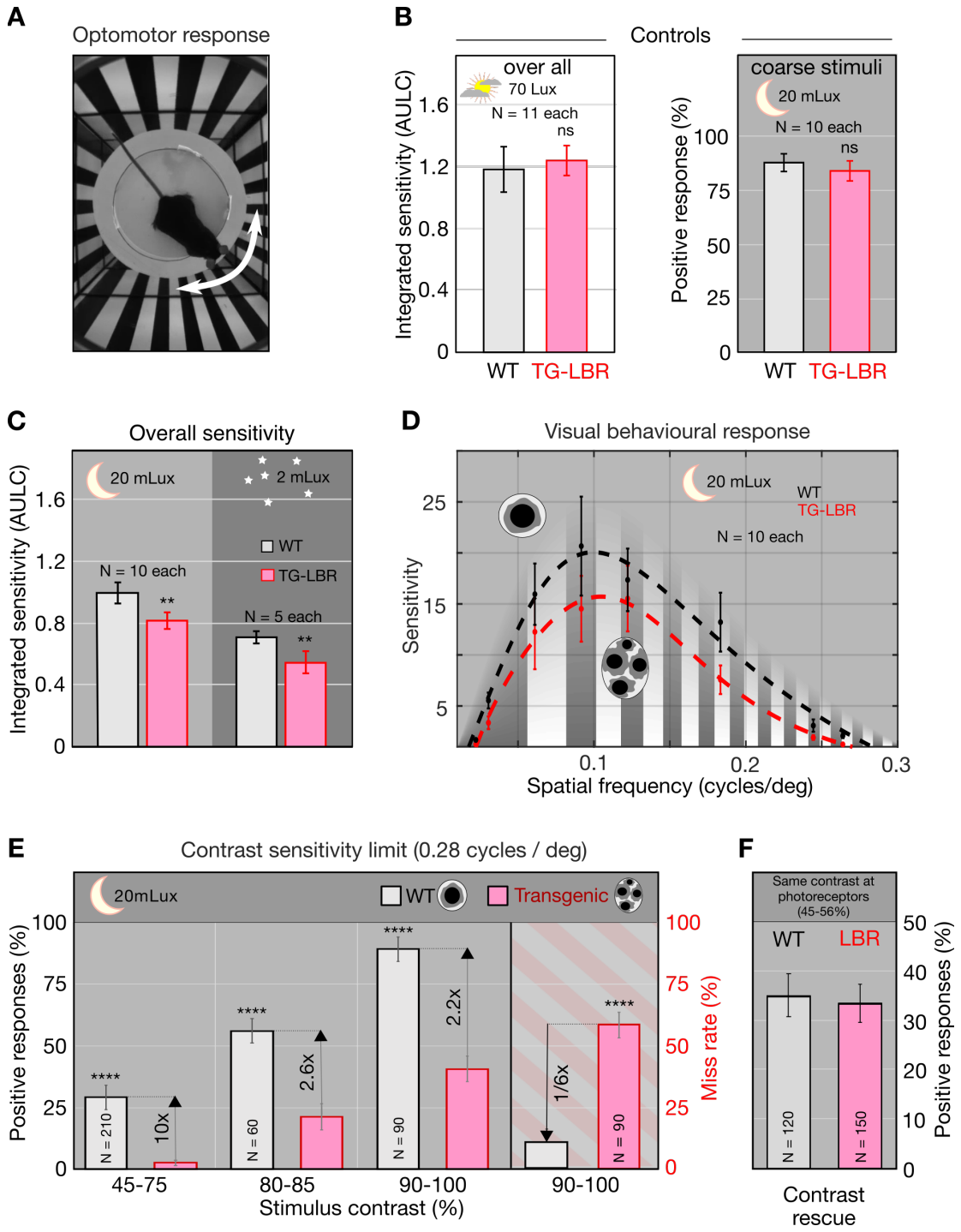

Fig. 4: Nuclear inversion improves contrast sensitivity in the dark. (A) Illustration of the automated optomotor response experiment to assess the visual performance of mice, shown a 0.06 cycles/deg. **(B)** Photopic control condition and scotopic coarse stimulus (0.06cycles/deg) control showing no significant difference between WT and TG-LBR mice. **(C)** Under scotopic conditions (20 and 2 mLux) the overall sensitivity of the WT mice is 22 and 29% higher than TG-LBR mice (area under log contrast sensitivity curve, AULC). mean+/- 95% CI, ($p < 0.01$) **(D)** Contrast sensitivity curves evaluated at 20mLux light intensity. Significant differences appear at angular sizes above 0.15 cycles/deg. **(E)** Behaviour differences are strongest for stimuli close to the visual threshold. Here the mice in possession of the inverted rod nuclei (WT) possess an up to 10 times higher sensitivity at intermediate contrasts (29% vs 3% correct response in 45-75% contrast range), and a 6 times reduced risk to miss a motion stimulus at high contrasts (10 vs 59% failure in detection, 0.26-0.3 cycles/deg), ($p<0.0001$) mean +/-s.d. N indicates number of individual trials of 10 animals together for each mouse type.

Acknowledgements: We would like to acknowledge the help from the following facilities at MPI-CBG - Biomedical Services, Cell technologies, Light Microscopy, Media Technologies & Outreach, Sequencing and Genotyping, Transgenic Core, during multiple phases of the project. The authors thank Jochen Guck, Elisabeth Knust, Caren Norden, Iain Patten, Marino Zerial and all the members of the Kreysing Lab for helpful discussions & comments. The authors thank Striatech GmbH for assistance in adapting the optomotor setup (OptoDrum) to scotopic light levels.

Author contributions: KS and MK designed the experimental setup and experiments. IS provided the TG-LBR transgenic mouse line. MA provided Rod-Cone (Rd1/Cpfl1) double KO & Rhodopsin KO mice. KS and MK designed optical experiments, which KS carried out. KS and MK and analyzed the data. HP assisted with FACS experiments. HP, AG, KS and IS recorded morphological data. MW and EWM performed computer simulations of light propagation. KS, OB, MK, and MA designed behavioral tests, which KS and OB carried out. KS wrote initial draft. All authors contributed to a critical discussion of the data and participated in writing the manuscript, which KS and MK finalized. MK coordinated the research.

Funding: The authors acknowledge the following funding sources Max-Planck-Gesellschaft (MPG): KS, MW, HP, AG, EWM, MK; Technische Universität Dresden (TU Dresden): OB, MA; Deutsche Forschungsgemeinschaft (DFG): OB, MA, funding from DFG, grant Nos. AD375/6-1, FZT111, EXC68; Bundesministerium für Bildung und Forschung (BMBF): KS, EWM, MK, 031L0044; Deutsche Forschungsgemeinschaft (DFG): IS, SO1054/3 and SFB1064. The funders had no role in study design, data collection and interpretation.

Competing interests: Authors declare no competing interests.

Ethics Statement: "All animal studies were performed in accordance with European and German animal welfare legislation (Tierschutzgesetz), the ARVO Statement for the Use of Animals in Ophthalmic and Vision Research, and the NIH Guide for the care and use of laboratory work in strict pathogen-free conditions in the animal

facilities of the Max Planck Institute of Molecular Cell Biology and Genetics, Dresden, Germany and the Center for Regenerative Therapies Dresden, Germany. Protocols were approved by the Institutional Animal Welfare Officer (Tierschutzbeauftragter) and the ethics committee of the TU Dresden. Necessary licenses were obtained from the regional Ethical Commission for Animal Experimentation of Dresden, Germany (Tierversuchskommission, Landesdirektion Sachsen)"

Data and materials availability: The authors declare that the data supporting the findings of this study are available within the paper and its supplementary information files.

References

Alam, N.M., Altimus, C.M., Douglas, R.M., Hattar, S., and Prusky, G.T. (2015). Photoreceptor regulation of spatial visual behavior. Invest. Ophthalmol. Vis. Sci. *56*, 1842–1849.

Artal, P., Chen, L., Fernández, E.J., Singer, B., Manzanera, S., and Williams, D.R. (2004). Neural compensation for the eye's optical aberrations. J Vis *4*, 281–287.

Banks, M.S., Sprague, W.W., Schmoll, J., Parnell, J.A.Q., and Love, G.D. (2015). Why do animal eyes have pupils of different shapes? Science Advances *1*, e1500391–e1500391.

Barlow, H.B. (1956). Retinal Noise and Absolute Threshold. J. Opt. Soc. Am., JOSA *46*, 634–639.

Benkner, B., Mutter, M., Ecke, G., and Münch, T.A. (2013). Characterizing visual performance in mice: an objective and automated system based on the optokinetic reflex. Behav. Neurosci. *127*, 788–796.

Boreman, G.D. (2001). Modulation Transfer Function in Optical and Electro-Optical Systems (1000 20th Street, Bellingham, WA 98227-0010 USA: SPIE).

Błaszczak, Z., Kreysing, M., and Guck, J. (2014). Direct observation of light focusing by single photoreceptor cell nuclei. Opt. Express, OE *22*, 11043–11060.

Chang, B., Hawes, N.L., Hurd, R.E., Davisson, M.T., Nusinowitz, S., and Heckenlively, J.R. (2002). Retinal degeneration mutants in the mouse. Vision Research *42*, 517–525.

Cronin, T.W., Johnsen, S., Marshall, N.J., and Warrant, E.J. (2014). Visual Ecology (Princeton University Press).

de Vries, H.L. (1943). The quantum character of light and its bearing upon threshold of vision, the differential sensitivity and visual acuity of the eye. Physica *10*, 553–564.

Dowling, J.E. (1987). The Retina (Harvard University Press).

Drezek, R., Guillaud, M., Collier, T., Boiko, I., Malpica, A., Macaulay, C., Follen, M., and Richards-Kortum, R. (2003). Light scattering from cervical cells throughout neoplastic progression: influence of nuclear morphology, DNA content, and chromatin texture. J. Biomed. Opt. *8*, 7–16.

Enoch, J.M. (1961). Nature of the transmission of energy in the retinal receptors. J. Opt. Soc. Am. *51*, 1122–1126.

Feodorova, Y., Koch, M., Bultman, S., Michalakis, S., and Solovei, I. (2015). Quick and reliable method for retina dissociation and separation of rod photoreceptor perikarya from adult mice. MethodsX *2*, 39–46.

Flevaris, A.V., and Murray, S.O. (2015). Attention Determines Contextual Enhancement versus Suppression in Human Primary Visual Cortex. J. Neurosci. *35*, 12273–12280.

Hess, R.F., and Dakin, S.C. (1988). The role of “contrast enhancement” in the detection and appearance of visual contours. Vision Research *38*, 783–787.

Hughes, A.E.O., Enright, J.M., Myers, C.A., Shen, S.Q., and Corbo, J.C. (2017). Cell Type-Specific Epigenomic Analysis Reveals a Uniquely Closed Chromatin Architecture in Mouse Rod Photoreceptors. Sci Rep *7*, 43184.

Humphries, M.M., Rancourt, D., Farrar, G.J., Kenna, P., Hazel, M., Bush, R.A., Sieving, P.A., Sheils, D.M., McNally, N., Creighton, P., et al. (1997). Retinopathy induced in mice by targeted disruption of the rhodopsin gene. Nat. Genet. *15*, 216–219.

Jaissle, G.B., May, C.A., Reinhard, J., Kohler, K., Fauser, S., Lütjen-Drecoll, E., Zrenner, E., and Seeliger, M.W. (2001). Evaluation of the rhodopsin knockout mouse as a model of pure cone function. Invest. Ophthalmol. Vis. Sci. *42*, 506–513.

Johnsen, S. (2012). The Optics of Life (Princeton University Press).

Kreysing, M., Boyde, L., Guck, J., and Chalut, K.J. (2010). Physical insight into light scattering by photoreceptor cell nuclei. Opt Lett *35*, 2639–2641.

Kyba, C., Mohar, A., and Posch, T. (2017). How bright is moonlight? A&G *58*.

Marina, O.C., Sanders, C.K., and Mourant, J.R. (2012). Correlating light scattering with internal cellular structures. Biomed. Opt. Express *3*, 296–312.

Mourant, J.R., Canpolat, M., Brocker, C., Esponda-Ramos, O., Johnson, T.M., Matanock, A., Stetter, K., and Freyer, J.P. (2000). Light scattering from cells: the

contribution of the nucleus and the effects of proliferative status. J. Biomed. Opt. *5*, 131–138.

Nagelberg, S., Zarzar, L.D., Nicolas, N., Subramanian, K., Kalow, J.A., Sresht, V., Blankschtein, D., Barbastathis, G., Kreysing, M., Swager, T.M., et al. (2017). Reconfigurable and responsive droplet-based compound micro-lenses. Nature Communications *8*, 14673.

Němec, P., Cveková, P., Burda, H., Benada, O., and Peichl, L. (2007). Visual systems and the role of vision in subterranean rodents: Diversity of retinal properties and visual system designs. In Subterranean Rodents: News From Underground, (Berlin, Heidelberg: Springer Berlin Heidelberg), pp. 129–160.

Nilsson, D.-E. (2009). The evolution of eyes and visually guided behaviour. Philosophical Transactions of the Royal Society B: Biological Sciences *364*, 2833–2847.

O'Carroll, D.C., and Warrant, E.J. (2017). Vision in dim light: highlights and challenges. Philos. Trans. R. Soc. Lond., B, Biol. Sci. *372*, 20160062.

Peichl, L. (2005). Diversity of mammalian photoreceptor properties: Adaptations to habitat and lifestyle? The Anatomical Record Part a: Discoveries in Molecular, Cellular, and Evolutionary Biology *287A*, 1001–1012.

Prusky, G.T., Alam, N.M., Beekman, S., and Douglas, R.M. (2004). Rapid Quantification of Adult and Developing Mouse Spatial Vision Using a Virtual Optomotor System. Invest. Ophthalmol. Vis. Sci. *45*, 4611–4616.

Prusky, G.T., West, P.W.R., and Douglas, R.M. (2000). Behavioral assessment of visual acuity in mice and rats. Vision Research *40*, 2201–2209.

Rose, A. (1948). The sensitivity performance of the human eye on an absolute scale. J. Opt. Soc. Am. *38*, 196–208.

Schmucker, C., and Schaeffel, F. (2004). A paraxial schematic eye model for the growing C57BL/6 mouse. Vision Research *44*, 1857–1867.

Shevell, S.K., Holliday, I., and Whittle, P. (1992). Two separate neural mechanisms of brightness induction. Vision Research *32*, 2331–2340.

Solovei, I., Kreysing, M., Lanctôt, C., Kösem, S., Peichl, L., Cremer, T., Guck, J., and Joffe, B. (2009). Nuclear architecture of rod photoreceptor cells adapts to vision in mammalian evolution. Cell *137*, 356–368.

Solovei, I., Wang, A.S., Thanisch, K., Schmidt, C.S., Krebs, S., Zwerger, M., Cohen, T.V., Devys, D., Foisner, R., Peichl, L., et al. (2013). LBR and lamin A/C sequentially tether peripheral heterochromatin and inversely regulate differentiation. Cell *152*, 584–598.

Thibos, L.N., Hong, X., Bradley, A., and Applegate, R.A. (2004). Accuracy and precision of objective refraction from wavefront aberrations. J Vis *4*, 329–351.

Thomas, K.N., Robison, B.H., and Johnsen, S. (2017). Two eyes for two purposes: in situ evidence for asymmetric vision in the cockeyed squids Histioteuthis heteropsis and Stigmatoteuthis dofleini. Philos. Trans. R. Soc. Lond., B, Biol. Sci. *372*, 20160069.

Tkatchenko, T.V., Shen, Y., and Tkatchenko, A.V. (2010). Analysis of postnatal eye development in the mouse with high-resolution small animal magnetic resonance imaging. Invest. Ophthalmol. Vis. Sci. *51*, 21–27.

Villegas, E.A., González, C., Bourdoncle, B., Bonnin, T., and Artal, P. (2002). Correlation between optical and psychophysical parameters as a function of defocus. Optom Vis Sci *79*, 60–67.

Warrant, E.J. (1999). Seeing better at night: life style, eye design and the optimum strategy of spatial and temporal summation. Vision Research *39*, 1611–1630.

Warrant, E., and Nilsson, D.-E. (2006). Invertebrate Vision (Cambridge University Press).

Warrant, E.J. (2017). The remarkable visual capacities of nocturnal insects: vision at the limits with small eyes and tiny brains. Philos. Trans. R. Soc. Lond., B, Biol. Sci. *372*, 20160063.

Warrant, E.J., and Locket, N.A. (2004). Vision in the deep sea. Biological Reviews *79*, 671–712.

Weigert, M., Subramanian, K., Bundschuh, S.T., Myers, E.W., and Kreysing, M. (2018). Biobeam-Multiplexed wave-optical simulations of light-sheet microscopy. PLoS Comput. Biol. *14*, e1006079.